

Absolute Experimental Cross Sections for the Ionization of Singly Charged Barium Ions by Electron Impact*

R. K. Feeney,[†] J. W. Hooper, and M. T. Elford[‡]

School of Electrical Engineering, Georgia Institute of Technology, Atlanta, Georgia 30332

(Received 18 May 1972)

The absolute cross sections for the single ionization of Ba⁺ ions by electron impact have been measured as a function of incident electron energy over the electron energy range from below threshold (10.001 eV) to approximately 1000 eV. It is found that the cross section increases from 1.94×10^{-16} to 3.76×10^{-16} cm² between 15.1 and 18 eV actual incident electron energy. This rapid rise is interpreted as the onset of autoionization. Some indication of structure occurring near the peak of the cross-section curve such as found in the isoelectronic system Cs is observed, but the relative magnitude of the apparent structure is of the same order as the 90% random-error confidence limits and thus cannot conclusively be regarded as being present. The maximum total error in the measurements is estimated to have its greatest value of less than $\pm 20\%$ at 15.5 eV while $\pm 12\%$ is typical of other energies. Of the total error, $\pm 7\%$ is deemed to be systematic. At incident electron energies below threshold, the cross section is found to be zero within 1% of the cross section at 48 eV. The measurements were performed in an all-metal ultrahigh-vacuum crossed-beam facility in which the nominal operating pressure was less than 5×10^{-9} Torr. The ion source was a water-cooled surface-ionization-type ion source while the electron source was a modified 6L6GC beam power tube. Continuous-beam techniques were used for the majority of the measurements, but modulated-beam methods were employed as a check. Measurements made by the two techniques agreed to well within the allowable experimental error and showed no systematic variations. Numerous consistency checks were performed to evaluate possible sources of experimental error such as pressure modulation of the background gas, focusing of the ion beam by the electron beam, and errors in the beam-profile determination. The present Ba⁺ ionization data are compared with the existing experimental and theoretical results.

I. INTRODUCTION

The absolute cross sections for the single ionization of Ba⁺ ions by electron impact have been measured as a function of incident electron energy from below threshold (10.001 eV) to approximately 1000 eV. This research was undertaken primarily to carefully examine the Ba⁺ ionization cross section for structure due to the effects of direct inner-shell ionization and autoionization. Direct ionization is the process whereby a valence or loosely bound inner-shell electron is removed in the ionization encounter. Autoionization is a decay process from quasibound excited states lying above the ionization threshold. The total ionization cross section is the sum of the partial cross sections for direct ionization and for autoionization. Since each of the processes that contribute to the total cross section has its individual magnitude and threshold energy, the total ionization cross section will exhibit a variation which depends upon the summation of the two.

The electron-impact ionizations for alkali metals heavier than Na exhibit well-defined double maxima. This feature is quite prominent and has been observed by a number of investigators¹⁻⁷; it is attributed to the onset of inner-shell direct ionization,⁸ to autoionization,³ or to a combination

of the two processes.^{6,7,9}

It is to be expected that these same processes are active in the electron-impact ionization of the isoelectronic alkaline earth ions. However, the manifestation of the processes might well be different because the electron binding energies and threshold laws for ionization and excitation are not the same for ions as for neutral atoms. The latter effect is of great importance because the threshold behavior for electron-impact excitation of ions is quite different from that for the excitation of neutral atoms,¹⁰⁻¹³ and therefore the onset of autoionization should be different for the two systems.

At the present time there are only a few experimental and theoretical results for the electron-impact ionization of the alkaline earth ions by electron impact. Cross sections for the electron-impact ionization of Mg⁺ have been measured by Martin *et al.*¹⁴ and those for Ba⁺ by Peart and Dolder.¹⁵ Theoretical calculations are also rather limited. Bely *et al.*¹⁶ have calculated the cross section for the ionization of Ba⁺ by electron impact. Mather *et al.*¹⁷ have calculated the cross sections for the ionization of Sr⁺ and Ba⁺ by electron impact using the classical-binary-encounter method of Thomas and Garcia.¹⁸ Bely¹⁹ has predicted structure due to autoionization in the sodiumlike isoelectronic

sequence. Moores and Nussbaumer²⁰ have calculated the electron-impact ionization of Mg^+ using the Coulomb-Born approximation with contributions due to inner-shell direct ionization and autoionization included. Their estimate of the autoionization contribution, although much less than that of Bely, is still in conflict with experiment, since Martin *et al.* could have detected variations in the cross section less than the predicted value. The results of Moores and Nussbaumer do seem to indicate that inner-shell direct ionization contributes significantly to the total ionization cross section. Details of the theoretical and experimental work concerned with the ionization of Ba^+ are included in a later section of this paper.

This paper presents a discussion of the experimental apparatus and method, a discussion of the consistency checks and experimental results, and a comparison with relevant theoretical and experimental results.

II. APPARATUS AND METHOD

The experimental method involves the use of a crossed-beam apparatus in which approximately monoenergetic beams of Ba^+ ions and electrons are caused to intersect at right angles in a well-defined collision region. The crossed-beam technique, which probably originates with the work of

Funk,²¹ has now become a well-established tool for the study of charged-particle-charged-particle collision processes. There have been several discussions of the advantages and difficulties inherent in charged-particle-charged-particle crossed-beam experiments and most of the early work utilizing this method has been critically evaluated.²²⁻²⁶ Accordingly, with the availability of such a complete body of reference material, a general discussion of the experimental technique will not be given here; only those unique problems associated with the present experiments are considered.

A schematic diagram of the experimental apparatus, which is a modified version of that developed by Lineberger *et al.*,²³ is given in Fig. 1. Singly charged barium ions are produced by a water-cooled surface-ionization-type ion source using a heated rhenium filament. Ions produced by the source pass through the several focusing, collimating, and deflecting structures and then into the interaction volume. A rectangular electron beam intersects the ion beam in the interaction region. Just prior to entering the interaction region the two beams pass through a scanner which determines their spatial profiles. After undergoing collisions with the electrons in the interaction region, the ion beam which now contains several charge states passes into the large parallel-plate

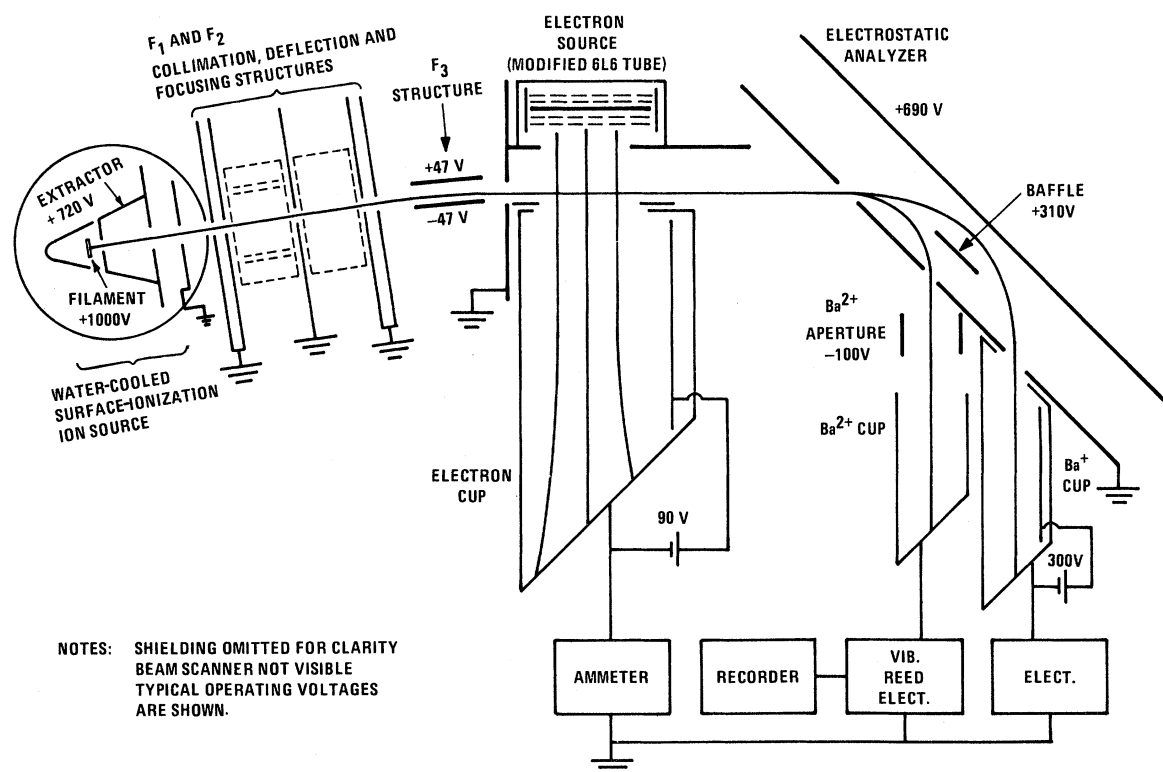


FIG. 1. Schematic diagram of the experimental apparatus.

electrostatic analyzer. Here the Ba^+ and Ba^{2+} beam components are separated and directed into their respective Faraday cups.

Although the experimental apparatus is basically the same as described by Lineberger *et al.*, a few significant modifications were made pursuant to the present work. The changes are summarized below.

A larger, but similar vacuum chamber was employed in this work. The cylindrical stainless-steel chamber is 51 cm high by 55 cm in diameter. The vacuum system employs a 15-cm oil diffusion pump and a zeolite molecular-sieve trap. The base pressure is about 1.5×10^{-9} Torr and the pressure with all sources operating is $(3-5) \times 10^{-9}$ Torr.

The thermionic-type source used previously was unable to produce Ba^+ ions and was replaced by a surface-ionization-type ion source. A surface-ionization source was chosen because of the requirement that the ion beam be in its ground state. Since the $5^2D_{3/2}$ and $5^2D_{5/2}$ metastable electronic energy levels lie only 0.6 and 0.7 eV, respectively, above the $6^2S_{1/2}$ ground state, it was necessary that the ion source have a small probability of exciting these levels. Measurements made during this work have shown that the surface-ionization barium-ion source produces negligible metastable contamination of the ion beam. The constructional and operational details of the ion source are discussed elsewhere.²⁷

The substitution of the surface-ionization-type ion source reduced the space available for ion-beam collimation and necessitated the addition of a third focus and deflection structure (F_1 in Fig. 1). This structure also serves to pulse the ion beam by deflecting it away from the structure exit aperture, when the experiment is operated in the pulsed-beam mode.

As in the original experiment, a type 6L6GC beam tetrode was used as an electron source. However, it was found that space-charge expansion of the electron beam precluded the use of a single electron-source configuration over the entire range of electron energies. Since the electron energy range below 100 eV was deemed most important in this experiment, the electron source was first optimized for that regime. This was accomplished by decreasing the preinteraction electron-beam path length 0.48 cm and removing the cant from the electron emitter. (The cant, which is discussed in the earlier work,²³ is a tilt about the axis of the electron beam imposed to increase the effective height of the electron beam.) When first operated under these conditions, it was noted that the electric field of the electron source penetrated into the interaction region. The origin of this field was found to be the beam-forming plates of the 6L6GC

tube, which with the cant removed were in a more exposed position. This field penetration was completely eliminated by decreasing the size of the exit aperture in the electron-source mounting bracket. The electron beam still completely clears the aperture, which is now approximately the size of the opening between the beam-forming plates. When operating in the 100–1000-eV regime, the cant was reimposed and preinteraction electron-beam path length restored to its original value; no other changes were made. With these changes, a satisfactory form factor could be obtained over the electron energy range 8–1000 eV. There was a range of overlap from about 100–300 eV where either electron-source geometry could be used. Thus, when the geometry was changed, measurements in this range served as a transfer check on the performance of the electron source.

The energy spread of the electron beam delivered by a similar 6L6GC vacuum-tube-type electron source has been measured by Bacon and Hooper²⁸ and found to be about 1.1-eV full width at half-maximum (FWHM). Bacon and Hooper also found the mean electron energy to be about 2 eV below that value set by the electron-beam power supply. Retarding potential measurements and the onset of autoionization in the present experiment appear to confirm these measurements.

The ion-beam analysis, collection, and measurement systems are essentially unchanged from the original design; the postinteraction charge-state components of the ion beam are separated by an inclined parallel-plate electrostatic analyzer and directed into their respective Faraday cups. The Ba^+ ion current is measured by a Keithley model 610R electrometer, while the Ba^{2+} ion current is measured with a Cary model 31 vibrating reed electrometer operating in the rate-of-charge mode. The estimated accuracy of measurement for the Ba^+ and the Ba^{2+} ion-beam components is better than ± 2 and $\pm 3\%$, respectively.

The electron collection and measurement system is also nearly identical with that used previously. The electron-source housing design was improved and the electron Faraday cup modified so as to provide clearance for the source-cooling-water feedthrough. The accuracy of the electron-current determination is considered to be better than $\pm 2\%$.

III. CONSISTENCY CHECKS AND EXPERIMENTAL RESULTS

The cross section for ionization of singly charged ions by electron impact is obtained from the observed experimental quantities by the relationship²³

$$\sigma_{12} = \frac{eV_i V_e}{2(V_i^2 + V_e^2)^{1/2}} \left[I_{SIG}^{2+} / \int_{-\infty}^{\infty} i(z)j(z) dz \right]. \quad (1)$$

In this equation V_i and V_e are the ion and electron velocities; $i(z)dz$ and $j(z)dz$ are the ion and electron currents passing through the region z to $z + dz$; I_{SIG}^{2+} is the total electric current of doubly charged ions produced by electron impact; and e is the magnitude of the electron charge. Equation (1) is usually written as

$$\sigma_{12} = \frac{I_{\text{SIG}}^{2+}}{JI^+} \frac{eV_i V_e F}{2(V_i^2 + V_e^2)^{1/2}}, \quad (2)$$

where

$$F = \int_{-\infty}^{\infty} i(z) dz \int_{-\infty}^{\infty} j(z) dz / \int_{-\infty}^{\infty} i(z) j(z) dz \quad (3)$$

and I^+ and J are the total ion and electron currents. All of the currents in Eq. (2) are directly measurable. The factor F , known as the form factor, is a functional defined on the ion- and electron-beam current-density distributions. The form factor is usually approximated by simultaneously scanning both beams with an L -shaped probe having coplanar slits.

In principle, once the form factor is approximated, it is simple to evaluate the cross section; however, in practice serious difficulties are encountered in the measurements of I_{SIG}^{2+} and F . The other parameters in Eq. (2) can be routinely evaluated assuming that proper precautions are taken in apparatus design and accurate instrumentation is used. However, in order to assure that the electron-impact ionization signal and the form factor are being measured correctly it is necessary to apply a series of consistency checks. Details of these checks applicable to charged-particle-charged-particle crossed-beam experiments are found elsewhere.^{23, 25, 26}

A. Consistency Checks

The variation of the measured cross section be-

low threshold is zero to within $\pm 3\%$ of the 48-eV value. The $\pm 3\%$ interval includes the scatter which results from the cross-section computation. Since the determination of the measured cross sections below threshold involves the arithmetic manipulation of numbers having nearly the same value, small random errors in the signal-component determinations can produce a substantial departure from the nominal zero value. Typically, the random scatter is several times larger than the mean value of cross sections below threshold. The average value of the measured cross sections below threshold is less than 1% of the 48-eV cross section and the ensemble of values from which they are obtained show no systematic trend; that is, positive and negative values occur with approximately equal frequency. The zero cross section below threshold leads to the following conclusions.

(i) The metastable $5^2D_{5/2}$ and $5^2D_{3/2}$ levels are not populated to any appreciable extent. If these levels were populated, a consistently positive cross section would have been noted at the 9-eV energy value since the "tail" of the electron energy distribution overlaps the ionization energy of these metastable states.

(ii) The ion beam is sufficiently well focused that there are no significant changes in the measured electron-impact ionization signal due to the additional focusing action of the electron beam.

(iii) There is no appreciable increase in the charge-stripped signal component due to pressure modulation of the chamber pressure by the electron beam, and thus the continuous-beam technique is valid.²²⁻²⁶

The degree of dependence upon electron current of the measured 48-eV cross section is shown in Fig. 2. The ion energy is 1.0 keV and the nominal ion current is 1×10^{-7} A. The size of the data points

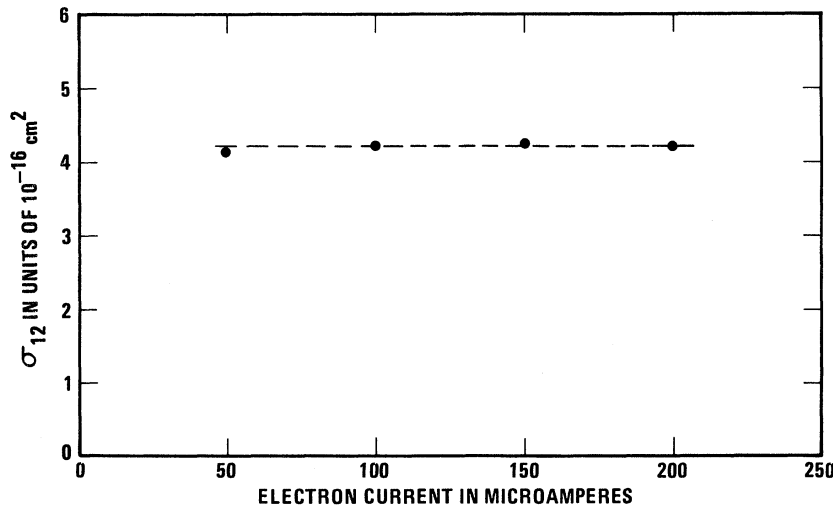


FIG. 2. Variation of the 48-eV cross section as a function of electron-beam current. The ion-beam energy is 1.0 keV and the ion current is 1×10^{-7} A.

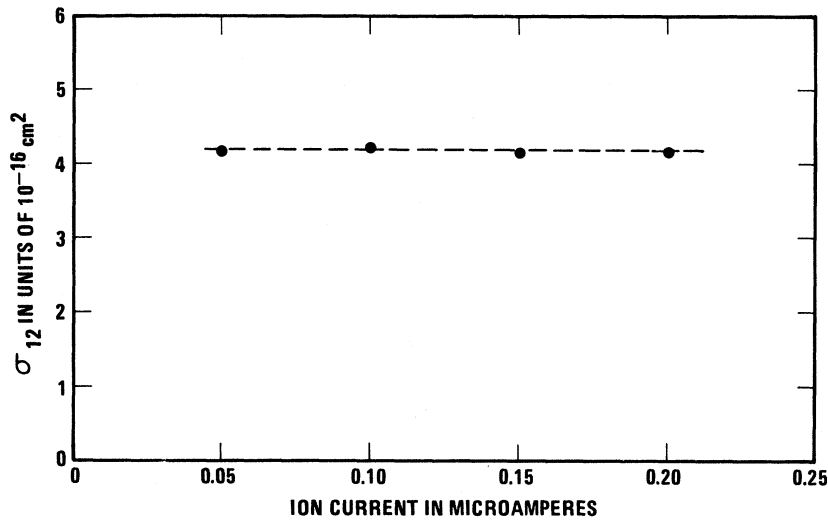


FIG. 3. Variation of the 48-eV cross section as a function of ion-beam current. The ion-beam energy is 1.0 keV and the electron-beam current is 100 μA .

is chosen to represent the typical short-term random error in the measurements. The variation of the cross section with electron current is well within the acceptable error for this experiment. An analysis of the cross section at 498 eV shows a similar lack of dependence upon electron current and is not presented.

The variation of the cross section at 48 eV as a function of the Ba^+ ion current is given in Fig. 3. The ion energy is 1000 eV and the electron current 100 μA . Again, there is no systematic dependence upon the test variable.

Figure 4 shows the variation of the cross section at 48 eV as a function of the form factor with all other parameters being held constant. The cross section is seen to be essentially independent of changes in the form factor except for the rolloff below about $F = 0.47$. This rolloff is a result of the

ion beam becoming too small to accommodate the space-charge spreading of the electron beam. All data were taken with form factors in the plateau region of the curve.

Table I shows the dependence of the measured cross section upon ion energy for several values of incident electron energy. Note that there is no systematic variation of the cross sections when the ion-beam energy is increased from the normally used value of 1.0 keV to 1.4 keV. This indicates that the deflection of the ion beam by the electron-beam space charge is not a problem of any significance, and therefore the electron-beam space charge does not adversely affect the measurement of the form factor.

B. Experimental Results

The absolute cross sections obtained with the

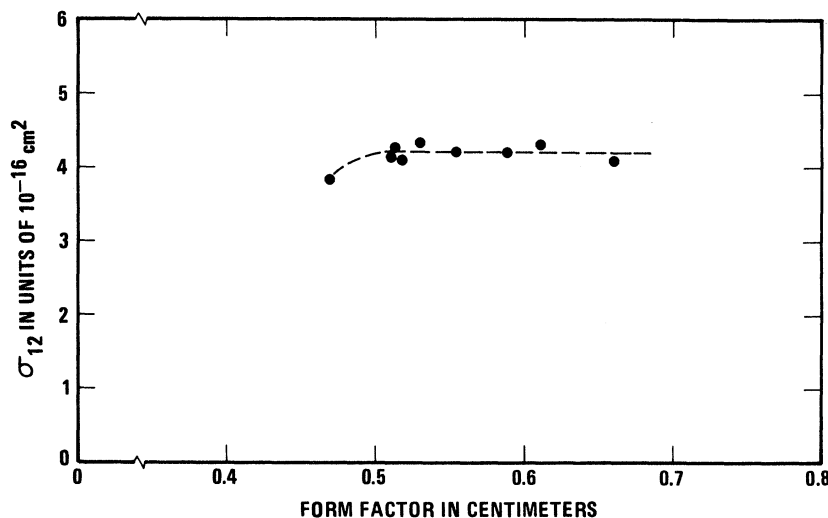


FIG. 4. Variation of the 48-eV cross section as a function of the form factor. The ion-beam energy is 1.0 keV, the ion-beam current is 1×10^{-7} , and the electron-beam current is 100 μA .

TABLE I. Dependence of σ_{12} upon ion energy at selected incident electron energies.

Indicated Electron Energy (eV)	Actual Electron Energy (eV)	Measured Cross Sections Units of 10^{-16} cm^2	
		1.0 keV Ions	1.4 keV Ions
50	48 ± 1	4.22	4.21
500	498 ± 2	1.64	1.66
700	698 ± 3	1.36	1.36

apparatus described above, operated in the continuous beam mode, are given in Table II and Fig. 5. Table II, the most complete presentation, gives the uncertainty in the electron energy, the experimental results, and a detailed breakdown of the experimental errors. Figure 5 presents all of the experimental data graphically, with the error bars reflecting the "maximum total error" as given in Table II.

Some additional comments relating to the experimental data are listed below.

(a) In all cases the actual measured values of the data are given; the data do not represent points derived from a smooth curve drawn as some "best fit" to the experimental points.

(b) All of the data presented were taken with 1.0-keV ions. Additional data taken with 1.4-keV ions were used only as a check; the results of this check were given previously in Table I.

(c) At least five valid measurements were taken at all energies with six to eight being typical. Additional measurements were made at the consistency-check electron energies of 8, 9, 48, 98, 298,

498, and 998 eV.

(d) The data represent only measurements made utilizing the continuous beam mode of operation. However, a comparison of measurements made by pulsed and continuous methods at selected incident electron energies is given in Table III. The pulsing scheme was similar to that developed by Dolder *et al.*,²⁹ except that the ion beam was pulsed with the smaller duty cycle.

C. Discussion of Errors

Systematic errors arise from the uncertainty in the electron-beam energy, the uncertainty in the ion-beam energy, and from the calibration of the measurement instruments.

As mentioned previously, the energy of the emitted electrons is estimated to be 2 ± 1 eV below the indicated electron acceleration energy with a FWHM of about 1.1 eV. The uncertainty in the electron energy caused by the internal oxide-cathode potential drop and the electron-acceleration-energy power-supply calibration are accounted for in the "actual electron energy" given in Table II. The 2-V energy degradation is reflected in Fig. 5, but the uncertainty in the electron energy is not. The effect of the finite width of the electron energy distribution is given qualitative consideration when comparison is made with theoretical predictions.

The estimated systematic error in the ion-beam energy is the sum of the error in the ion-beam acceleration potential and the voltage drop across the ionizing filament. This results in an ion-beam energy error of less than 1%. Since the measured cross section varies with the ion velocity and hence as the square root of the ion energy, the systematic error in the cross-section measurement due to this cause is less than 0.5%. As the estimate of the instrumentation error is thought to be con-

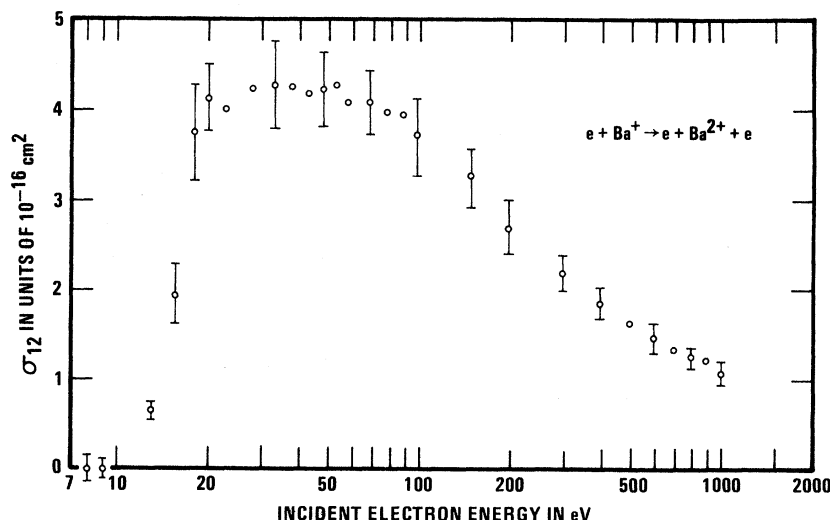


FIG. 5. Absolute experimental cross sections for the single ionization of Ba^+ ions by electron impact.

servative, the small component of systematic error due the ion-beam energy is not included in the total systematic error.

The errors of the measurement instruments are

combined to yield the worst-case estimate of the over-all error. This figure of $\pm 7\%$ is taken to be the systematic error of the instrumentation and the total systematic error.

TABLE II. Absolute experimental cross sections for the single ionization of Ba⁺ ions by electron impact.

Indicated Electron Energy, eV	Actual Electron Energy, eV	Cross Section Units 10^{-16} cm ²	90 Percent Confidence Limits, Percent	Maximum Experimental Scatter, Percent	Maximum Systematic Error, Percent	Maximum Total Error, Percent
10	8 ± 1	0.0	-	-	-	-
11	9 ± 1	0.0	-	-	-	-
15	13 ± 1	0.66	±8	+5 -9	±7	+12 -16
17.5	15.5 ± 1	1.94	±6	+12 -9	±7	+19 -16
20	18 ± 1	3.76	±6	+8 -9	±7	+15 -16
22	20 ± 1	4.12	±2	±2	±7	±9
25	23 ± 1	4.02	±2	+3 -5	±7	+10 -12
30	28 ± 1	4.24	±2	±3	±7	±10
35	33 ± 1	4.29	±3	+5 -4	±7	+12 -11
40	38 ± 1	4.26	±2	±3	±7	±10
45	43 ± 1	4.20	±3	+6 -5	±7	+13 -12
50	48 ± 1	4.22	±1	±3	±7	±10
55	53 ± 1	4.29	±3	+7 -6	±7	+14 -13
60	58 ± 1	4.09	±2	+3 -4	±7	+10 -11
70	68 ± 1	4.10	±1	±2	±7	±9
80	78 ± 1	3.97	±3	+4 -2	±7	+11 -9
90	88 ± 1	3.94	±2	±3	±7	±10
100	98 ± 1	3.72	±2	+4 -5	±7	+11 -12
150	148 ± 1	3.28	±2	+2 -4	±7	+9 -11
200	198 ± 2	2.69	±3	+4 -3	±7	+11 -10
300	298 ± 2	2.20	±1	±2	±7	±9

Table II. (Continued)

Indicated Electron Energy, eV	Actual Electron Energy, eV	Cross Section Units 10^{-16} cm ²	90 Percent Confidence Limits, Percent	Maximum Experimental Scatter, Percent	Maximum Systematic Error, Percent	Maximum Total Error, Percent
400	398 ± 2	1.87	±2	±2	±7	±9
500	498 ± 2	1.64	±1	±4	±7	±11
600	598 ± 3	1.49	±1	±3	±7	±10
700	698 ± 3	1.36	±2	+3 -5	±7	+10 -12
800	798 ± 3	1.27	±1	+2	±7	±9
900	898 ± 3	1.23	±3	+2 -4	±7	+9 -11
1000	998 ± 4	1.08	±5	+6 -5	±7	+13 -12

Two estimates of the random error were adopted for this work. The first and most conservative estimate of the random error is the extreme limits of the experimental scatter. This formulation suffers from the defect of producing an error that is likely to increase with the number of measurements (samples) at a given electron energy. Since a primary purpose of this research was to examine the cross sections for a possible structure, it was deemed necessary to use some statistical estimate of how closely the sample mean approaches the population mean. Such an estimate facilitates a more meaningful analysis of the relative shape of the cross-section curve. The 90% confidence limits of the mean³⁰ were adopted as the appropriate statistical parameter and are given in Table II.

When consideration was given to the absolute magnitude of the cross sections, the more conservative approach of setting the maximum total error equal to the sum of the maximum experimental scatter and the systematic error was adopted. This maximum total error is given in Table II and Fig. 5.

IV. COMPARISON WITH EXPERIMENT AND THEORY

The ionization of Ba⁺ ions by electron impact has been previously measured by Peart and Dolder.¹⁵ A meaningful comparison with their experimental results is complicated by minor inconsistencies in their tabulated and graphical data. However, the authors³¹ indicated that their tabulated data were correct and any ambiguities should be resolved in

favor of such data. Figure 6 presents a comparison between the present data and that of Peart and Dolder. The limits of maximum total experimental error are given for a representative sample of data points. The agreement between the two sets of data is generally quite good and is well within the combined experimental errors. The largest discrepancy, which occurs near 17-eV incident electron energy, is still within the combined exper-

TABLE III. Comparison of measurements made by pulsed and continuous methods at selected incident electron energies.

Indicated Electron Energy (eV)	Actual Electron Energy (eV)	Measured Cross Sections Units of 10^{-16} cm ²	
		Continuous	Pulsed
10	8 ± 1	0.0	0.0
25	23 ± 1	4.02	4.00
50	48 ± 1	4.22	4.32
150	148 ± 1	3.28	3.26
500	498 ± 2	1.64	1.63
700	698 ± 3	1.36	1.37
1000	998 ± 4	1.08	1.04

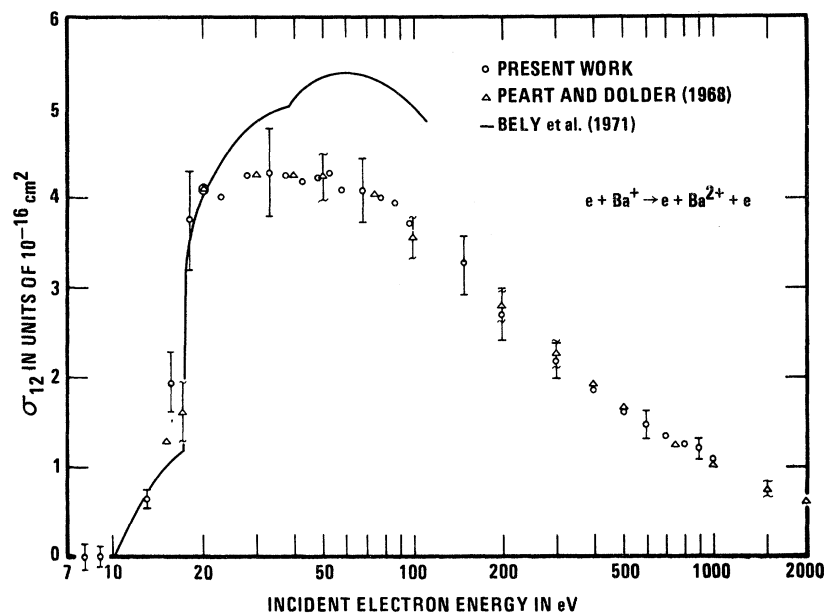


FIG. 6. Comparison of the present experimental results for the ionization of Ba^+ ions with some other experimental and theoretical data.

imental error when the combined uncertainty in electron energy of ± 3 eV is included.

Bely *et al.*¹⁶ have calculated the ionization cross sections for the ionizations of Ba^+ by electron impact from threshold to about 100 eV. The direct ionization contribution to the total ionization cross section was computed according to the Coulomb-Born II method. A comparison between their work and the two experimental results is also given in Fig. 6. Reasonable qualitative agreement is indicated, and the average absolute agreement of within about 25% is to be considered quite good for the approximations involved in the calculations. The onset of autoionization from the $(5p^5 6s 5d)^2 P$ level at 17.2 eV agrees well with both sets of experimental results when the spread and uncertainty in the electron-beam energy is considered.

Examination of the experimental cross section near the threshold for direct $5p$ ionization does not reveal the sharp and distinct break predicted by Bely *et al.* The experimental data do seem to convey some indication of systematic structure, but the magnitude of the variations is smaller than the 90% confidence limits and cannot conclusively be regarded as being present. It thus appears that the estimate of the $5p$ ionization cross section is perhaps too large, a fact that is consistent with the usual behavior of the Born-type calculations near threshold.

Mathur *et al.*¹⁷ attribute the sudden rise in the cross section to be due to direct ionization from the $5p$ subshell. Their calculations, which include direct ionization contributions from the first four subshells, were made with the modified clas-

sical-binary-encounter model of Thomas and Garcia.¹⁸ Their results are in good agreement with the experimental data near the peak of the cross section but the agreement becomes progressively worse as the incident electron energy is increased. At 1000 eV, the calculated cross section is about 50% of the measured value.

In the course of the present work, the electron-impact cross sections were calculated according to the classical method of Gryzinski.³² It was found that these results were strongly dependent upon the choice of the ionization energies used for the inner shells. By careful choice of ionization energies (usually incorrect) it was possible to generate structure in the cross section. In addition, it was noted that various empirical "focusing factors"³³ could be applied to the Gryzinski theory in such a manner as to improve the agreement near threshold; however, the agreement at high incident electron energies was not improved. The final calculation made with the inner-shell ionization energies estimated by McFarland³⁴ and including no correction for focusing was about 50% of the measured cross section at 1000 eV.³⁵ Classically scaled cross sections for the ionization of Cs were also found to be about 50% of the measured Ba^+ ionization cross section at 1000 eV.³⁵

ACKNOWLEDGMENTS

The authors are pleased to thank M. O. Pace and J. C. Majure for their helpful discussions.

*This work was partially supported by the Controlled Thermonuclear Research Program of the U. S. Atomic Energy Commission.

†The work reported here is a portion of a research program undertaken by one of us (R. K. F.) in partial fulfillment of the requirements for the degree of Doctor of Philosophy at the Georgia Institute of Technology.

‡Work performed while a Visiting Professor at the Georgia Institute of Technology. Present address: Australian National University, Canberra, A. C. T., Australia.

¹J. P. Tate and P. T. Smith, *Phys. Rev.* **46**, 733 (1934).

²Y. Kaneko, *J. Phys. Soc. Japan* **16**, 2288 (1961).

³G. O. Brink, *Phys. Rev.* **127**, 1204 (1962).

⁴G. O. Brink, *Phys. Rev.* **134**, A345 (1964).

⁵R. H. McFarland and J. D. Kinney, *Phys. Rev.* **137**, A1058 (1965).

⁶H. Heil and B. Scott, *Phys. Rev.* **145**, 279 (1966).

⁷K. J. Nygaard, *J. Chem. Phys.* **49**, 1995 (1968).

⁸J. D. Garcia, *J. Chem. Phys.* **47**, 3679 (1967).

⁹R. H. McFarland, *Phys. Rev.* **139**, A40 (1965).

¹⁰S. Geltman, *Topics in Atomic Collision Theory* (Academic, New York, 1969), pp. 152–159.

¹¹O. Bely and G. Van Regemorter, *Ann. Rev. Astron. Astrophys.* **8**, 329 (1970).

¹²B. L. Moiseiwitsch and S. J. Smith, *Rev. Mod. Phys.* **40**, 238 (1968).

¹³M. O. Pace, Ph. D. thesis (Georgia Institute of Technology, 1970) (unpublished).

¹⁴S. O. Martin, B. Peart, and K. T. Dolder, *J. Phys. B* **1**, 537 (1968).

¹⁵B. Peart and K. T. Dolder, *J. Phys. B* **1**, 872 (1968).

¹⁶O. Bely, S. B. Schwartz, and J. L. Val, *J. Phys. B* **4**, 1482 (1971).

¹⁷K. C. Mathur, A. N. Tripathi, and S. K. Joshi,

Intern. J. Mass Spectrom. Ion Phys. **4**, 483 (1970).

¹⁸B. K. Thomas and J. D. Garcia, *Phys. Rev.* **179**, 94 (1969).

¹⁹O. Bely, *J. Phys. B* **1**, 23 (1968).

²⁰D. L. Moores and H. Nussbaumer, *J. Phys. B* **3**, 161 (1970).

²¹H. Funk, *Ann. Physik* **4**, 149 (1930).

²²G. H. Dunn, in *Atomic Physics*, edited by B. Bederson, V. W. Cohen, and F. M. J. Pichanick (Plenum, New York, 1969), pp. 417–433.

²³W. C. Lineberger, J. W. Hooper, and E. W. McDaniel, *Phys. Rev.* **141**, 151 (1966).

²⁴J. W. Hooper, W. C. Lineberger, and F. M. Bacon, *Phys. Rev.* **141**, 165 (1966).

²⁵M. F. A. Harrison, *Brit. J. Appl. Phys.* **17**, 371 (1966).

²⁶K. T. Dolder, in *Case Studies in Atomic Collision Physics*, edited by E. W. McDaniel and M. R. C. McDowell (North-Holland, Amsterdam, 1969), Vol. I, pp. 251–330.

²⁷R. K. Feeney, F. M. Bacon, M. T. Elford, and J. W. Hooper, *Rev. Sci. Instr.* **43**, 549 (1972).

²⁸F. M. Bacon, and J. W. Hooper, *Phys. Rev.* **178**, 182 (1969).

²⁹K. T. Dolder, M. F. A. Harrison, and P. C. Thonemann, *Proc. Roy. Soc. (London)* **A264**, 367 (1961).

³⁰R. S. Burington and D. C. May, Jr., *Handbook of Probability and Statistics with Tables*, 2nd ed. (McGraw-Hill, New York, 1970).

³¹B. Peart (private communication).

³²M. Gryzinski, *Phys. Rev.* **138**, A336 (1965).

³³A. Burgess and I. C. Percival, *Advan. At. Mol. Phys.* **4**, 109 (1968).

³⁴R. H. McFarland, *Phys. Rev.* **159**, 20 (1967).

³⁵R. K. Feeney, Ph. D. thesis (Georgia Institute of Technology, 1970) (unpublished).